

Manganese Enhanced Magnetic Resonance Imaging

Jung Hee Lee and Alan P. Koretsky*

Laboratory of Functional and Molecular Imaging, National Institutes of Neurological Disorders and Stroke, NIH, Bethesda, MD, USA

Abstract: Manganese is an essential metal that participates as a co-factor in a number of critical biological functions such as electron transport, detoxification of free radicals, and synthesis of neurotransmitters. Like other heavy metals, high concentrations of manganese are toxic. For example, chronic overexposure to manganese leads to movement disorders. In order to maintain this balance between being an essential participant in enzyme function and being a toxic heavy metal, a rich biology has evolved to transport and store manganese. Paramagnetic forms of manganese ions are potent MRI relaxation agents. Indeed, Mn^{2+} was the first contrast agent proposed for use in MRI. Recently, there is renewed interest in combining the strong MRI relaxation effects of Mn^{2+} with its unique biology in order to expand the range of information that can be measured by MRI. Manganese Enhanced MRI is being developed to give unique tissue contrast, assess tissue viability, act as a surrogate marker of calcium influx into cells and trace neuronal connections. In this article we review recent work and point out prospects for the future uses of manganese enhanced MRI.

INTRODUCTION

In 1973, Paul Lauterbur published his seminal paper entitled, "Image formation by induced local interactions: examples employing nuclear magnetic resonance" [1]. This paper laid down the basic strategy that has evolved into modern MRI. Explicit in the title was the notion that a new type of imaging was proposed, one that relied on direct monitoring of induced local interactions, in this case the magnetic resonance frequency of water hydrogen atoms in an externally applied magnetic field gradient. At the time of Lauterbur's work, the notion to image water distribution seemed to be limited for medical applications because water density varied by only a small degree in tissues. However, by that time there were already results that demonstrated that magnetic resonance relaxation times of water were different in different tissues and might be altered by pathology [2]. To demonstrate that relaxation times could affect the intensity of images acquired using his new imaging strategy, Lauterbur used the well known ability of the paramagnetic ion, Mn^{2+} to alter the longitudinal relaxation time of water [1]. Thus, in one paper, Lauterbur demonstrated a new imaging technique and a strategy to alter contrast with exogenous agents. Today there are over 60 million MRI exams per year and approximately 25% rely on adding contrast [3].

The vast majority of the clinically useful MRI contrast is gadolinium based, however, there has been a renewed interest in the use of Mn^{2+} as contrast agent in MRI of animal models. This recent work is motivated by the growing interest in developing MRI techniques that are sensitive to specific molecular processes. Mn^{2+} is a co-factor for a number of enzymes, including superoxide dismutase and glutamine synthetase [4, 5]. As an essential heavy metal there are specific proteins for the transport of Mn^{2+} . Mn^{2+}

can enter cells using some of the same transport systems as Ca^{2+} [6-8] and it can bind to a number of intracellular sites because it has high affinity for Ca^{2+} , and Mg^{2+} binding sites on proteins and nucleic acids. When oxidized to Mn^{3+} , it can mimic iron and bind to transferrin and be stored in ferritin [9].

The rich biology of Mn^{2+} combined with its ability to act as an MRI contrast agent offers a large number of possibilities for using Manganese Enhanced MRI (MEMRI) to probe tissue function. Work has been performed demonstrating that MEMRI may be useful to report on cell viability [10, 11]. The activity of brain and heart has been monitored with MEMRI due to the ability of Mn^{2+} to enter excitable cells on voltage gated calcium channels [12-16]. When applied to specific regions of the brain, Mn^{2+} will be transported in an anterograde direction and cross synapses allowing non-invasive tracing of brain connections with MRI [17-20]. Finally, Mn^{2+} accumulates differently in sub-regions of different tissues leading to MRI contrast that gives a high degree of anatomical detail [21-23]. Here we review this recent work using MEMRI and discuss some future prospects.

SYSTEMIC ADMINISTRATION OF MANGANESE LEADS TO USEFUL MRI CONTRAST

The earliest work with Mn^{2+} as an MRI contrast agent, relied on giving a systemic dose of Mn^{2+} (usually as the chloride salt) and monitoring distribution in a number of tissues [24, 25]. Indeed, Mn^{2+} accumulates in almost all tissues when administered either intravenously, intraperitoneally, or intramuscularly. Significant accumulation was detected in many tissues such as liver, kidney, heart and brain [24-27]. At least two important points came from work looking at tissue enhancement with Mn^{2+} . First, based on the fact that tissue enhancement lasts long after blood enhancement and that the volume distribution is more like an intracellular agent, it is generally accepted that MRI contrast

*Address correspondence to this author at the LFMI, NINDS, Building 10, BID118, 10 Center Drive, Bethesda, MD 20812, USA; Tel: 301 402- 9659; Fax: 301 480-2558; E-mail: koretskya@ninds.nih.gov

after systemic MnCl_2 comes from intracellular Mn^{2+} [24-28]. Thus, systemically administered Mn^{2+} accumulates intracellularly as opposed to chelated gadolinium based MRI contrast agents that remain extracellular. Proof that Mn^{2+} readily enter cells also comes from NMR spectroscopy. Fig. 1C shows a ^{31}P NMR spectrum from an exposed sheep heart. Peaks due to ATP, phosphocreatine and inorganic phosphate are readily detected. Intravenous administration of MnCl_2 led to a broadening of the phosphate containing metabolites due to the binding of Mn^{2+} and shortening of the T_2 relaxation time (Fig. 1B). Indeed this effect gets so large that the phosphate peaks broaden beyond detection under the NMR conditions used (Fig. 1A) [29]. This happens due to direct binding of Mn^{2+} to the intracellular metabolites inside the heart cells. Broadening of phosphorus containing metabolites has been reported from the perfused rat heart as well [30, 31]. The ability of Mn^{2+} to broaden NMR peaks has been used to follow the compartmentation of Mn^{2+} in yeast, where most of the Mn^{2+} is sequestered in the vacuole [32]. A time course of broadening of first extracellular phosphates, followed by cytosolic phosphates and finally vacuolar phosphates enabled the rates of Mn^{2+} transport in these compartments to be studied [32]. Thus, the working assumption, and an exciting aspect of analyzing MEMRI based contrast, is that the Mn^{2+} is intracellular.

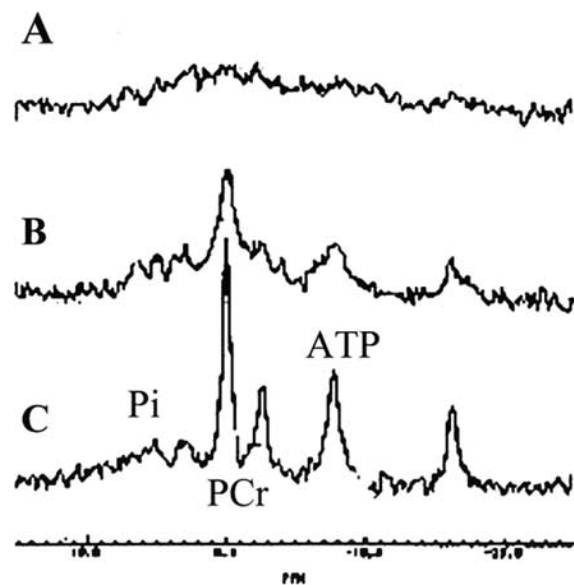


Fig. (1). ^{31}P NMR spectra from a surgically exposed sheep heart before (C), during (B) and after (A) infusion of MnCl_2 . The intracellular phosphorus containing metabolites, inorganic phosphate (Pi), phosphocreatine (PCr), and ATP broaden until they cannot be detected due to direct binding of the paramagnetic Mn^{2+} as it enters the cardiac myocytes.

The second important conclusion from work on systemically administered Mn^{2+} as an MRI contrast agent was that it could be used to assess normal tissue function by imaging the uptake of Mn^{2+} . Normal uptake into a tissue implies normal function and some abnormalities, for example a

tumor or ischemia, should be detected due to differential uptake of Mn^{2+} . The use of Mn^{2+} as an MRI contrast has been inhibited due to the fact that the doses needed to cause changes large enough to be detected in early studies was toxic in the animal models tested [26]. However, the goal to measure tissue function was pursued by making chelates of Mn^{2+} . Manganese dipyridoxaldiphosphate (MnDPDP) is presently FDA approved for liver imaging for negative enhancement of tumors in the liver [33]. In addition, there has been much work demonstrating the usefulness of MnDPDP for imaging cardiac ischemia [10, 11, 28, 34]. While a detailed description of work with MnDPDP is beyond the scope of this review, it is interesting to note that much of the Mn^{2+} comes off of the chelate slowly after administration [35]. This means that some of the tissue enhancement detected with MnDPDP was due to Mn^{2+} .

The toxicity of Mn^{2+} , especially its well known ability to cause movement disorders in people that are chronically overexposed [36], has led to much interest in using MRI to image the areas of the brain that accumulate high levels of Mn^{2+} . Work has been performed in rat [37, 38], monkeys [39], and humans [40], which demonstrated that there is accumulation of Mn^{2+} in basal ganglia and other areas of the brain after administration of Mn^{2+} . High levels of Mn^{2+} in basal ganglia can lead to cell death and cause the Parkinson like symptoms associated with chronic manganese exposure. In addition to helping elucidate the pathophysiology associated with manganese, this work also has led to the notion that systemic administration of Mn^{2+} might be a simple way to enhance MRI images of the brain. Indeed, recent work in rat and mouse show that doses of MnCl_2 that due not have toxic effects lead to useful contrast for MRI of the brain [21-23, 41].

Fig. 2 shows examples of T_1 weighted MRI images from the rat and mouse brain illustrating the anatomical detail available twenty-four hours after an intravenous administration of MnCl_2 . Enhancement of the dentate gyrus and CA formation of the hippocampus can be detected. In addition, deep nuclei can be imaged, as illustrated by the heterogeneous contrast detected in the rat brain image. The mouse brain image illustrates that almost all areas of the brain enhance. Largest enhancement is detected in the olfactory bulb, hippocampus and cerebellum [21-23, 41]. However, there is large accumulation in many deep brain structures as well. Initially after systemic administration of Mn^{2+} there is large accumulation in the choroid plexus and subventricular tissue. The enhancement moves into CSF space and then throughout the brain, while the choroid plexus and CSF return to pre- Mn^{2+} intensities [21, 23]. The pattern of MRI enhancement evolves for about twenty-four hours after intravenous administration of MnCl_2 and then reaches the distribution illustrated in Fig. 2. This distribution remains constant but the enhancement steadily decreases over a two-week period. The fact that Mn^{2+} enhancement can last a long time in a tissue after administration may be a useful property.

At high resolution many details of neuroarchitecture can be detected with MEMRI. Fig. 3 shows that distinct layers in the olfactory bulb and cortex can be detected [22, 23]. To the best of our knowledge this is the first imaging technique that gives such exquisite neuroanatomical detail throughout the

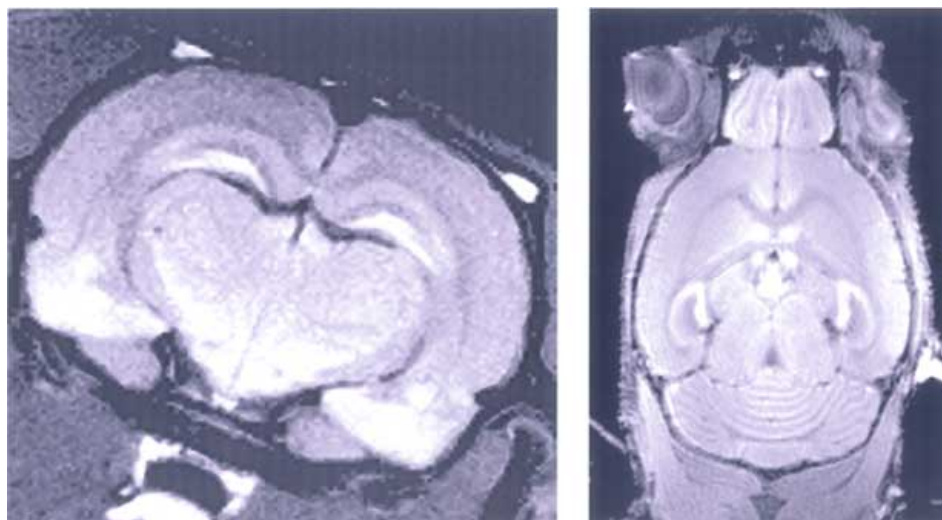


Fig. (2). Manganese Enhanced MRI of a rat brain (left) and a mouse brain (right) twenty-four hours after intravenous infusion of MnCl_2 . Strong enhancement is detected throughout the brain but higher levels of enhancement in some deep brain nuclei, hippocampus, olfactory bulb, and cerebellum lead to clear delineation of these structures. The rat brain image was acquired on a 4.7T MRI and the mouse brain image on an 11.7T MRI. In both cases T_1 weighted, spin echo images were acquired with a short repetition time of 300 msec. In-plane image resolution is approximately 150 microns with a 500 micron slice thickness in the rat and for the mouse image the resolution was approximately 100 micron isotropic. Adapted from reference 23 and unpublished data courtesy of J.H. Lee.



Fig. (3). Manganese Enhanced MRI of the rat brain twenty-four hours after intravenous infusion of MnCl_2 . A) MEMRI showing a slice through the brain at the level of the somatosensory cortex. Laminar heterogeneity of intensities can be detected in the cortex (arrow) which are assigned to specific cortical layers. B) MEMRI showing a slice through the brain at the level of the olfactory bulb. Again heterogeneity of intensities can be detected that correspond to specific layers in the olfactory bulb. Images were obtained on an 11.7T MRI using a T_1 weighted spin echo MRI sequence at approximately 100 micron resolution. Adapted from reference 23.

brain, non-invasively. An interesting area for further work will be in delineating why Mn^{2+} leads to such interesting contrast in the brain. To first approximation, the regions of the brain that have the largest enhancement also have the highest cell density and it may be that cell density alone controls the final contrast. In the sections below we discuss the fact that Mn^{2+} can accumulate in cells based on activity

and so the activity level of different regions may determine the distribution. Finally, Mn^{2+} has differential affinity for different cell organelles and different proteins and this may dictate the distribution of Mn^{2+} . Understanding the cellular factors responsible for the enhancement detected in the brain may lead to the use of MEMRI to image changes in these factors.

Systemic administration of Mn^{2+} is useful for imaging other tissues as well. There has been some work imaging the heart after intravenous administration of Mn^{2+} in order to compare to MnDPDP [10, 11, 28]. The normal heart rapidly uptakes Mn^{2+} and it can be predicted that low flow regions of the heart would take up less Mn^{2+} leading to an indicator of ischemia. Indeed, MEMRI has been used to detect ischemia in both the intact and perfused rat and guinea pig heart [10, 11, 28]. Recently, this type of work was extended to the dog heart [42]. Fig. 4 shows T_1 weighted images of heart before, during and after $MnCl_2$ infusion. In these images the pre- Mn^{2+} signal intensity is intentionally set close to zero using inversion recovery so that the images are heavily T_1 weighted. Immediately after infusion of Mn^{2+} , the blood in the ventricles and the heart is enhanced. After about 20 minutes the blood returns to pre- Mn^{2+} levels due to rapid clearance of the infused Mn^{2+} . However, the normal heart tissue remains enhanced compared to the blood due to the intracellular accumulation of Mn^{2+} . Using this type of protocol an ischemic region that was induced by ligating the left ascending aorta could be readily detected due to low levels of enhancement after infusion of $MnCl_2$ [42]. In the mouse heart, the enhancement associated with administration of the Mn^{2+} lasted for at least two days [16] and probably lasts much longer. The stability of the intracellular Mn^{2+} contrast means that an event, such as cardiac ischemia can be encoded by administering Mn^{2+} and then MRI performed later. In this way, MEMRI has memory. Many other tissues such as the pancreas, kidney, pituitary, as well as the liver are known to accumulate Mn^{2+} . It will be interesting to see if systemic administration of Mn^{2+} to perform MEMRI of these tissues leads to useful contrast for imaging anatomical structure in these tissues.

MEMRI CAN BE USED TO LOCALIZE ACTIVITY

As discussed above, manganese can enter cells and there are a number of transport systems that can carry manganese. One of the most interesting class of transporters that is known to carry Mn^{2+} are voltage-gated calcium transporters

[6-8]. These are key transporters in excitable cells such as neurons or myocytes because they open to allow calcium to enter when cells depolarize. Thus, voltage gated calcium channels offer a way to have Mn^{2+} accumulate in cells based on the activity of the cell. Indeed, in isolated cells the rate that Mn^{2+} enters has been measured by monitoring the quenching of fluorescent calcium indicators by Mn^{2+} [43]. This rate of fluorescence quenching has been used as a surrogate marker to quantitate calcium influx in a variety of cells [44]. With this in mind, Lin *et al.* developed what they termed Activation Induced Manganese Enhanced MRI or AIM MRI to monitor activity in the brain of rodents [12]. The idea was to perform an intravenous infusion of Mn^{2+} while activating the brain pharmacologically or with somatosensory stimulation. Activation should lead to increased Mn^{2+} influx on voltage gated calcium channels and thus increased MRI contrast on T_1 weighted images.

Glutamate, amphetamines, somatosensory activation, and awakening from anesthesia all led to large increases of signal in the appropriate regions of the brain [12, 21]. In order to get sufficient accumulation it was necessary to open the blood-brain barrier with mannitol. The Mn^{2+} accumulated in active regions on a short time scale (minutes) but once accumulated did not leave for at least two hours. Fig. 5 shows AIM MRI on the somatosensory system of a rat. In this case the forepaw and whiskers were stimulated and enhancement was detected in the appropriate somatosensory regions of the cortex as well as the relevant thalamic regions. In addition, enhancement in the ventricles could be detected due to the intravenous infusion of $MnCl_2$. In this case the rat had been stimulated outside the MRI and then MRI was performed within half an hour illustrating that Mn^{2+} accumulation remained even after activity stopped. This clearly illustrates the memory capability of MEMRI. In this case the local activity of the brain was encoded by infusing Mn^{2+} at the time of stimulation but imaged at a later time. The fact that Mn^{2+} enters rapidly but does not leave rapidly is thus an advantage and disadvantage. The disadvantage is that rapid changes in activity cannot readily be followed with

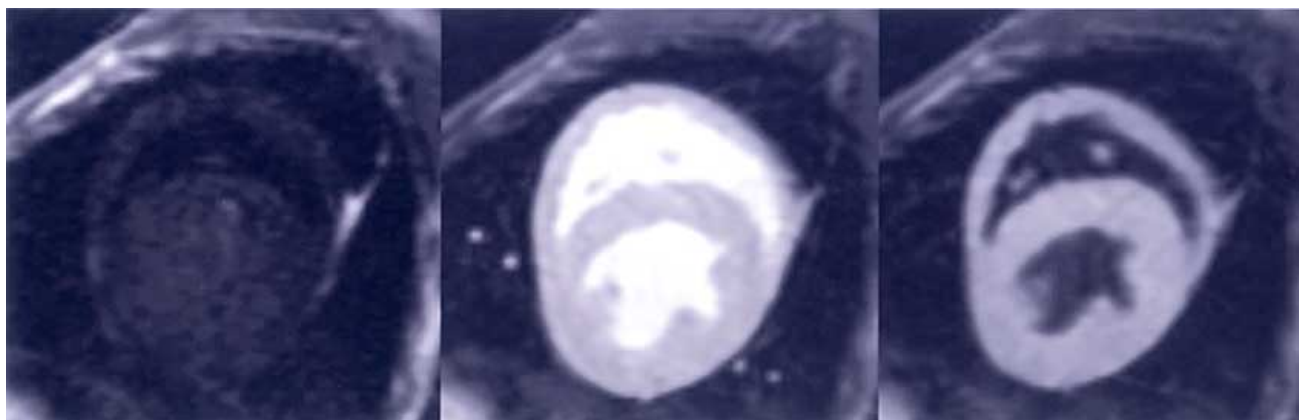


Fig. (4). Manganese Enhanced MRI of the canine heart before (left), during (middle) and 30 minutes after a bolus infusion of $MnCl_2$. T_1 weighted images were acquired on a 1.5T MRI using an inversion recovery spin echo with an in plane resolution of 1 mm and a slice thickness of 8mm. Inversion times were set so as to null signal from tissue and blood prior to infusion of $MnCl_2$. During infusion of $MnCl_2$ bright signal is detected in blood and heart but by 30 minutes the blood is back to pre- $MnCl_2$ intensities but the tissue remains enhanced. Adapted from reference 42.

AIM MRI. The advantage is that Mn^{2+} can be given outside the MRI and an image of activity can be frozen at the time of Mn^{2+} infusion. Thus it may be possible to give Mn^{2+} to animals while they are behaving in a complex environment. A first step was demonstrated when Mn^{2+} was given to an awake animal and then imaged under anesthesia to demonstrate activity patterns at the time of delivery of Mn^{2+} [12].

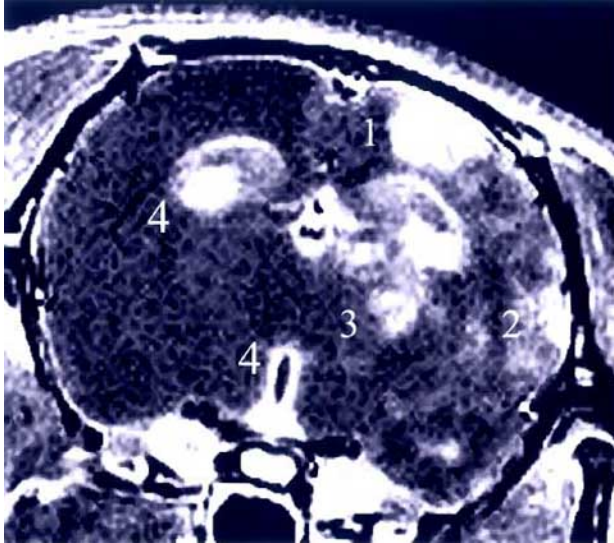


Fig. (5). Activation Induced Manganese Enhanced MRI of the rat brain. High signal intensity can be detected in the forepaw somatosensory area (1), the whisker somatosensory area (2), and the thalamus (3) due to direct stimulation of the forepaw and whiskers during infusion of $MnCl_2$ in the presence of a broken blood brain barrier. Signal intensity in ventricular regions (4) are due to uptake of $MnCl_2$ into the CSF space and periventricular tissue. For this rat, infusion of $MnCl_2$ and stimulation were performed outside the MRI and the imaging was performed within an hour. Imaging was performed on a 4.7T MRI using a T_1 weighted spin-echo sequence. Adapted from reference 21.

AIM MRI has been performed on the somatosensory system of the rat to compare to the more common, hemodynamic based functional MRI techniques (fMRI) [13]. The results indicated that the regions mapped by AIM MRI were roughly the same as with fMRI. AIM MRI had a distribution with higher intensity in layer 4 as opposed to fMRI that detected a higher intensity near the surface where large draining veins are located. This result indicates that because AIM MRI is sensitive to calcium influx rather than hemodynamic changes associated with neuronal activity it may offer a whole brain imaging tool more closely associated with neural activity. Recent work has demonstrated a dynamic AIM MRI technique for the brain that helps reduce non-specific signals associated with AIM MRI [14]. In addition to somatosensory and pharmacological stimulation, a recent paper demonstrated activation of hypothalamic nuclei involved in osmoregulation [15]. The localization of hypothalamic activation detected by AIM MRI showed good correspondence to that detected with expression of *cfos*. The fact that AIM MRI is sensitive to calcium influx also opens opportunities for studying pathophysiology. An exciting

recent result demonstrated this by using AIM MRI to image the excitotoxic phase of stroke [45]. In this case Mn^{2+} was infused just prior to performing a stroke in the rat. A large increase in contrast was detected a few minutes after the stroke. This was interpreted to be due to influx of Mn^{2+} reporting on the large calcium influx that occurs when there is a large release of glutamate caused by the stroke. It will be interesting to compare AIM MRI views of damaged tissue compared to diffusion and perfusion MRI techniques.

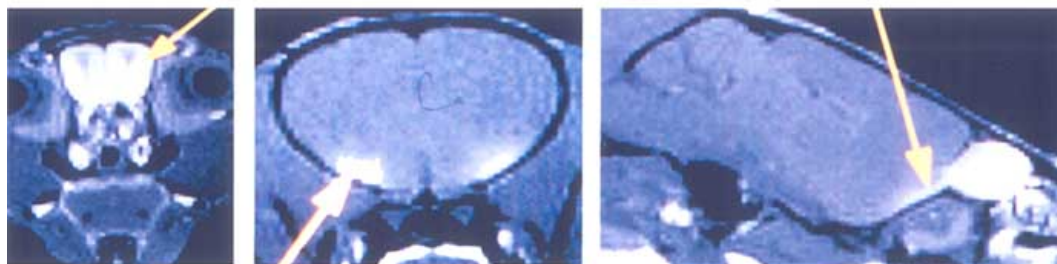
AIM MRI has been demonstrated on other tissues. In the mouse heart the rate of Mn^{2+} accumulation was shown to increase with positive inotropic agents that stimulate calcium influx and decrease with calcium channel blockers [16]. Similarly in the perfused heart it has been demonstrated that calcium channel blockers inhibit Mn^{2+} influx [8, 31, 46]. The ability of AIM MRI to be sensitive to cardiac inotropy opens possibilities for distinguishing viable from non-viable myocardium and to assess the calcium sensitivity of contraction. Many other tissues should be amenable to AIM MRI where a ligand or electrical activity cause an influx of calcium into cells.

TRACING NEURONAL CONNECTIONS WITH MEMRI

The third property of Mn^{2+} that makes it very useful for MRI of the brain is that it will move along appropriate neuronal pathways. Studies have demonstrated this by using radioactive isotopes of Mn^{2+} to follow the olfactory pathway in fish and after injection into the rat brain [47, 48]. These studies were designed to determine how environmental Mn^{2+} enters the food supply and the mechanism for Mn^{2+} distribution in the brain. The combination of the excellent MRI contrast properties of Mn^{2+} and the fact that it moves in neurons was first used to perform MEMRI neuronal tracing in the mouse olfactory and visual pathway [17]. Pautler *et al.* injected concentrated $MnCl_2$ solutions into the nose and eye of mice and performed MRI for up to 48 hours after injection. MRI enhancement moved from the turbinates to the olfactory bulb and out of the bulb to the primary olfactory cortex. In the eye, MRI enhancement moved down the optic nerve and then into the brain where enhancement of the superior colliculus could be detected [17]. Fig. 6 shows an example of the MEMRI tract tracing in the olfactory and visual system of the mouse.

In addition to tracing neuronal connections, MEMRI can give specific anatomical information. Indeed, one can use the track tracing properties of Mn^{2+} to selectively enhance structures of interest. Indeed, in Fig. 6 specific brain structures such as the primary olfactory cortex and superior colliculus are well defined. Thus, the track tracing properties of Mn^{2+} enabled the functional architecture to be revealed based on connectivity. The ability to trace neuronal connections non-invasively at such high resolution is a unique property of MEMRI neuronal tracing. Diffusion MRI techniques can follow white matter tracks *in vivo* [49], however, they haven't shown the same potential for functional connectivity that MEMRI exhibits. Of course, the major advantage of diffusion MRI tracing techniques is that they are now readily applied in humans. It is not clear whether MEMRI tracing techniques can be used in humans.

A) Olfactory Pathway



B) Visual Pathway

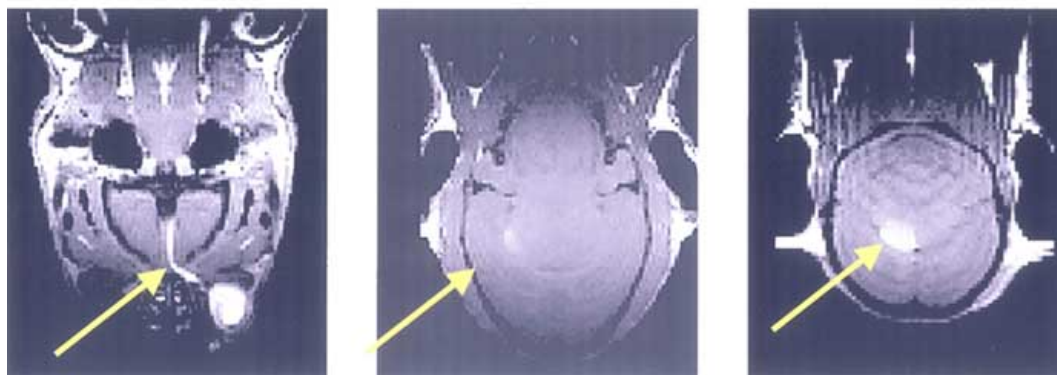


Fig. (6). Tracing of the mouse olfactory and visual pathway with Manganese Enhanced MRI. A) Sections through a three dimensional MRI image of a mouse brain, 36 hours after pipetting $MnCl_2$ into the nose. Bright intensity can be detected in the olfactory bulb (left) and the primary olfactory cortex (middle). A longitudinal view shows enhancement from the bulb and tracking back to the olfactory cortex (right). B) Sections through a three dimensional MRI image of a mouse brain, 36 hours after injecting $MnCl_2$ directly into the eye. Enhancement along the optic nerve (left), into the brain (center) and up to the superior colliculus (right) is readily detected. Images were acquired on a 7T MRI using a T_1 weighted spin-echo sequence at approximately 90 micron isotropic resolution. Adapted from reference 17.

The fact that MRI enhancement moves out of the olfactory bulb into the primary olfactory cortex demonstrates that Mn^{2+} can cross synapses. The rate of enhancement along the optic nerve was found to move at 2 mm/hour, consistent with Mn^{2+} being moved by a fast axonal transport process. Furthermore, follow-up studies showed that calcium channel blockers and microtubule disrupting agents blocked the MRI enhancement in the olfactory system [50]. Taken together these results argue that Mn^{2+} first enters neurons on voltage gated calcium channels (the property used for AIM MRI). Once inside of cells, the hypothesis is that the Mn^{2+} gets packaged into vesicles that can be transported down an axon. One possibility is that Mn^{2+} moves into endoplasmic reticulum (ER) on a recently described Mn^{2+}/Ca^{2+} transporter, PMR1 [51], and then is mixed in vesicles as they bud off the ER. Another possibility is that Mn^{2+} can be transported directly into vesicles, for example on the heavy metal transporter, DMT1 [52]. A final possibility is that Mn^{2+} binds to another molecule that binds or is transported into vesicles. All results to date indicate that Mn^{2+} moves in an anterograde direction which implies that the Mn^{2+} is entering a subset of vesicles in the cell. To cross a synapse, Mn^{2+} must be released and then uptake by the postsynaptic cell. If

Mn^{2+} is packaged in vesicles that contain neurotransmitter then it is easy to envision release into the synapse. Uptake can occur on voltage gated calcium channels on the postsynaptic side. The rate of transport down the axon argues that the transport is the rate limiting process. However, this requires further experimentation. A rate limitation at the synapse might make it possible to use MEMRI to measure changes in synaptic strength.

A number of groups have extended the use of MEMRI for imaging neuronal networks. Similar results described above after injection into the mouse eye have been obtained in the rat [18]. In the rat the innervation of many visual areas was detected, however, there was no evidence of trans-synaptic transport in these studies. It will be interesting to see whether the tracing properties of Mn^{2+} are general for different neural systems. Using MRI to measure the transport of Mn^{2+} down the optic nerve has been shown to be a sensitive indicator of damage to the nerve due to radiation [53]. This result clearly indicates that there will be many useful applications of MEMRI tracing to study damage and repair of neural connections. The fact that MEMRI so clearly enhances specific neuronal pathways in the brain opens up possibilities for verifying and extending the important

diffusion based MRI tracing techniques. Two studies have demonstrated this nice combination of MRI techniques to show that diffusion tensor imaging agrees with MEMRI tracing in the visual system of the rat [54, 55].

Recently, it has been demonstrated in the bird [19], the monkey [20], and the rat [56] that direct injections of small volumes of $MnCl_2$ into the brain can be used to trace connections. In the bird injection into one of the song centers led to delineation of the other centers connected to the injected site [19]. This enabled an anatomical measurement of these centers that normal MRI could not otherwise detect. Exciting preliminary data indicates that Mn^{2+} tracing of the song center will be sensitive to changes in size and connectivity of these centers during exposure to specific songs or testosterone [57, 58]. In the monkey, a careful comparison was made between MEMRI track tracing and another anterograde tracer, horse-radish peroxidase [20]. The two techniques were in agreement, in addition, the authors were able to follow the Mn^{2+} through multiple synapses indicating that extensive neural networks can be traced. Similar results imaging Mn^{2+} movement across multiple synapses was obtained from the rat after injection of Mn^{2+} into the amygdala and striatum [56].

Our working model is that Mn^{2+} first enters neurons on voltage gated calcium channels and then is transported in an anterograde direction. This opens up a truly unique experimental design for tracing neuronal connections. It should be possible to have Mn^{2+} accumulate in a specific set of active neurons and then trace their connections. This strategy has recently been demonstrated in the olfactory system of mice [50]. In this case a mouse was exposed to Mn^{2+} and a specific odor so as to cause Mn^{2+} to accumulate in the subset of olfactory neurons in the nose that were activated by the odor. MRI was performed 1.5 hours after

exposure to enable the Mn^{2+} to move into the olfactory bulb enabling the representation of the odor to be mapped. Fig. 7 shows the results for two odors, a pheromone that caused enhancement in the accessory olfactory bulb and amyl acetate which enhances a region of the bulb in agreement with previous mapping using radiotracer techniques. This result opens up interesting possibilities for having Mn^{2+} accumulate in specific regions when they are active and then tracing anterograde connections from these specific areas.

CONCLUSIONS

There is rapidly increasing interest in developing MRI agents that give information about the specific distribution of a molecule or information about a specific biological process [59]. Part of the driving force for this interest in molecular imaging with MRI are the large number of interesting mouse models that are increasingly being analyzed by imaging techniques [60]. It has become clear that the rich biology of Mn^{2+} combined with its potent MRI relaxation properties is leading to exciting new opportunities to probe biological processes in animal models. Presently there are three ways to productively use MEMRI. First, simple systemic administration of Mn^{2+} leads to interesting and useful anatomical MRI contrast. The accumulation of Mn^{2+} is enabling analysis of anatomical structures by MRI that would otherwise be difficult to detect. The biological basis for the movement of Mn^{2+} into tissues and its final distribution needs to be more fully determined and this may lead to opportunities for new imaging strategies.

One well established way for Mn^{2+} to enter cells is on voltage gated calcium channels. This has enabled work with MEMRI to probe activity in brain and heart and the general strategy should be useful for a number of other tissues. Further work needs to be performed to clarify exactly which

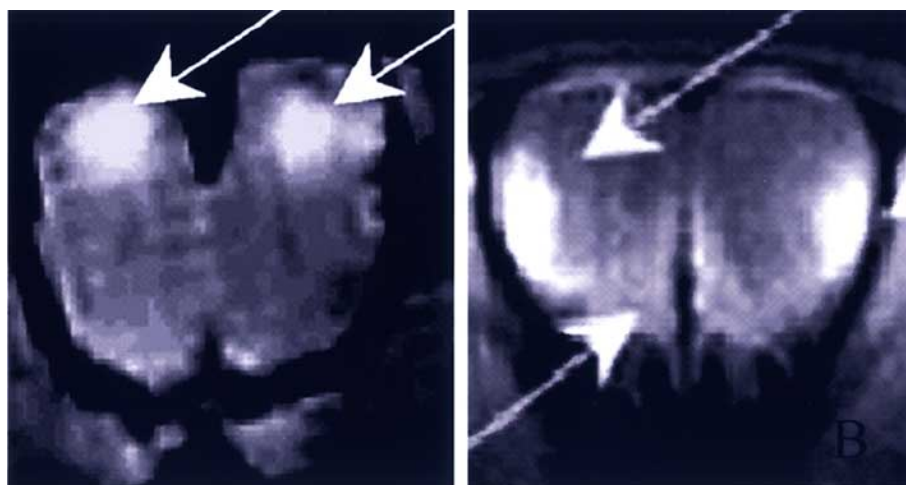


Fig. (7). Mapping odors onto the olfactory bulb using manganese enhanced MRI. The ability to accumulate $MnCl_2$ into an active area and then trace connections is illustrated for the olfactory system. Mice were exposed to $MnCl_2$ and either: A) high pheromone content odor, or B) amyl acetate and MRI was performed 1.5 hours after exposure. Initial accumulation of Mn^{2+} occurred in olfactory neurons in the turbinates that responded to the specific odor. Enhancement shown in the bulb developed 1.5 hours after exposure to the odor due to transport of the Mn^{2+} . Enhanced areas correspond to regions of the bulb known to be activated by the odors used. The images were obtained on a 7T MRI using a T_1 weighted spin-echo sequence at approximately 90 micron resolution. Adapted from reference 50.

channels Mn^{2+} can move through to enable AIM MRI to become a quantitative surrogate of calcium influx. There are no widely used non-invasive imaging techniques that monitor the influx of this important second messenger and therefore, there are many opportunities to study the quantitative control of Ca^{2+} influx in intact functioning tissues.

The ability of MEMRI to trace neuronal connections is opening up numerous possibilities for non-invasively imaging neural networks. This should enable changes in the brain of an individual animal to be studied before and after a broad range of perturbations such as learning, plasticity, injury and repair. The combination of the ability to control the accumulation of Mn^{2+} in one region of the brain based on activity and then image the connections from that area should open novel strategies to study functional connectivity in the brain with MEMRI.

A major challenge for the development of MEMRI is to increase sensitivity so that lower doses of Mn^{2+} can be used. Presently the doses used in animals are higher than what can be used in humans. However, a factor of 10 gain in the ability to detect Mn^{2+} would make it possible to use MEMRI in humans. Most of the intensity changes being used in MEMRI experiments are on the order of 50-100%. Functional MRI experiments so widely used to map activity in the brain routinely rely on 2-5% changes in MRI intensities. Increasing sensitivity to Mn^{2+} to this level will make the broad range of information available from MEMRI in animal models available to help diagnosis, stage, and determine treatment efficacy for human disease.

ACKNOWLEDGEMENTS

Special thanks go to Y.J. Lin Wu, A. Silva, T. Hu, B. Roman, I. Aoki, for their hard work developing MEMRI in the laboratory. Thanks also to J. Bulte for the kind invitation to submit this work and his patience in editing. Support for the work comes from the Intramural Research Program, NINDS directed by Eugene Major and Henry McFarland.

REFERENCES

- [1] Lauterbur, P.C. (1973) *Nature* **242**, 190-191.
- [2] Damadian, R. (1971) *Science* **171**, 1151-1153.
- [3] Haen, C. (2001) *Topics in Magn. Resonan. Imag.* **12**, 221-230.
- [4] Li, Y., Huang, T., Carlson, E., Melov, S., Ursell, P., Olson, J., Noble, L., Yoshimura, M., Berger, C. and Chan, P. (1995) *Nat. Genet.* **11**, 376-381
- [5] Wedler, F. and Denman, R. (1984) *Curr. Top. Cell Regul.* **24**, 153-169.
- [6] Drapeau, P. and Nachsen, D. (1984) *J. Physiol.* **348**, 493-510.
- [7] Narita, K., Kawaski, F. and Kita, H. (1990) *Brain Res.* **510**, 289-295.
- [8] Hunter, D., Haworth, R., Berkoff, H. (1981) *J. Mol. Cell. Cardiol.* **13**, 823-832.
- [9] Aschner, M. and Aschner, J. (1990) *Brain Res. Bull.* **24**, 857-860.
- [10] Wendland, M., Saeed, M., Lund, G. and Higgins, C. (1999) *J. Magn. Resonan. Imag.* **10**, 694-702.
- [11] Brurok, H., Skoglund, T., Berg, K., Skarra, S., Karlsson, J., Jynge, P. (1999) *NMR Biomed.* **12**, 364-372.
- [12] Lin, Y. and Koretsky, A. (1997) *Magn. Resonan. Med.* **38**, 378-388.
- [13] Duong, T., Silva, A., Lee, S. and Kim, S. (2000) *Magn. Resonan. Med.* **43**, 383-392.
- [14] Aoki, I., Tanaka, C., Takegami, T., Ebisu, T., Umeda, M., Fukunaga, M., Fukuda, K., Silva, A., Koretsky, A., Naruse, S. (2002) *Magn. Resonan. Med.* **48**, 927-933.
- [15] Morita, H., Ogino, T., Seo, Y., Fujiki, N., Tanaka, K., Takamata, A., Nakamura, S. and Murakami, M. (2002) *Neurosci. Lett.* **326**, 101-104.
- [16] Hu, T., Pautler, R., MacGowan, G. and Koretsky, A. (2001) *Magn Resonan. Med.* **46**, 884-890.
- [17] Pautler, R., Silva, A. and Koretsky, A. (1998) *Magn. Resonan. Med.* **40**, 740-748.
- [18] Watanabe, T., Michaelis, T. and Frahm, J. (2001) *J Magn Resonan. Med.* **46**, 424-429.
- [19] Van Der Linden, A., Verhoye, M., Van Meir, V., Tindemans, I., Eens, M., Absil, P. and Balthazart, J. (2002) *J. Neuroscience* **112**, 467-474, 2002
- [20] Saleem, K., Pauls, J., Augath, M., Trinath, T., Prause, B., Hasjikawa, T. and Logothetis, N. (2002) *Neuron* **34**, 685-700.
- [21] Lin, Y. (1997) "MRI of the rat and mouse brain after systemic administration of $MnCl_2$." Thesis, Carnegie Mellon University, Pittsburgh, PA.
- [22] Watanabe, T., Natt, O., Boretius, S., Frahm, J. and Michaelis, T. (2002) *Magn. Resonan. Med.* **48**, 852-859.
- [23] Aoki, I., Lin-Wu, Y., Silva, A., Lynch, R. and Koretsky, A. (2004) *Neuroimage* **22**, 1046-1059.
- [24] Lauterbur, P., Mendonca Dias, M., Rudin, A. (1978) "Augmentation of tissue water proton spin-lattice relaxation rates by *in vivo* addition of paramagnetic ions." In: *Frontiers of Biological Energetics*, Dutton, P., Leigh, J. and Scarpa, A. eds. Academic Press, NY Volume **1**, pp752-759.
- [25] Hollis, D., Bulkley, B. and Nunnally, R. (1978) *Clin. Res.* **26**, 240A.
- [26] Wolf, G. and Baum, L. (1983) *Am. J. Roentgenol.* **141**, 193-197.
- [27] Kang, Y. and Gore, J. (1984) *Invest. Radiol.* **19**, 399-407.
- [28] Saeed, M., Higgins, C., Geschwind, J. and Wendland, M. (2000) *Eur. Radiol.* **10**, 310-318.
- [29] Koretsky, A., Detre, J., Williams, D.S. and Ho, C. (1988) Unpublished observation.
- [30] Nunally, R. and Hollis, D. (1979) *Biochemistry* **18**, 3642-3646.
- [31] Elst, L., Colet, J. and Muller, R. (1997) *Invest. Radiol.* **32**, 581-588.
- [32] Castro, C., Koretsky, A. and Domach, M. (1999) *Biotechnol. Prog.* **15**, 65-73.
- [33] Federle, M., Chezmar, J., Rubin, D., Weinreb, J., Freeny, P., Semelka, R., Brown, J., Borello, J., Lee, J., et al. (2000) *J. Magn Resonan. Imag.* **12**, 186-197.
- [34] Bremerich, J., Saeed, M., Arheden, H., Higgins, C. and Wendland, M. (2000) *Radiology* **216**, 524-530.
- [35] Gallez, B., Bacic, G. and Swartz, H. (1996) *Magn. Resonan. Med.* **35**, 14-19.
- [36] Barbeau, A. (1984) *Neurotoxicology* **5**, 13-35.
- [37] London, R., Toney, G., Gabel, S. and Funk, A. (1989) *Brain Res. Bull.* **23**, 229-235.
- [38] Wan, X, Fu, T., Smith, P., Brainard, J. and London, R. (1991) *Magn. Resonan. Med.* **21**, 97-106.
- [39] Newland, M., Ceckler, T., Kordower, J. and Weiss, B. (1989) *Exp. Neurol.* **106**, 251-258.
- [40] Lucchini, R., Albin, E., Placidi, D., Gasparotti, R., Pigozzi, M., Montani, G. and Alessio, L. (2000) *Neurotoxicology* **21**, 769-775.
- [41] Natt, O., Watanabe, T., Boretius, S., Radulovic, J., Frahm, J., Michaelis, T. (2002) *J. Neurosci. Methods* **120**, 203-209.
- [42] Hu, T., Christian, T., Aletas, A., Taylor, J., Koretsky, A. and Arai, A. (2002) *Int. Soc. Magn. Resonan. Med.* **9**, 654.
- [43] Hallam, T. and Rink, T. (1985) *FEBS Lett.* **186**, 175-179.
- [44] Shibuya, I. and Douglas, W. (1993) *Cell Calcium* **14**, 33-44.
- [45] Aoki, I., Ebisu, T., Tanaka, C., Katsuta, K., Fujikawa, A., Umeda, M., Fukunaga, M., Takegami, T., Shapiro, E. and Naruse, S. (2003) *Magn. Resonan. Med.* **50**, 7-12.
- [46] Nordhay, W., Anthonen, H., Bruvold, M., Jynge, P., Krane, J. and Brurok, H. (2003) *NMR Biomed.* **16**, 82-95.
- [47] Tjalve, H., Henriksson, J., Tallkvist, B., Larsson, B. and Lindquist, N. (1996) *Pharmacol. Toxicol.* **79**, 347-356.
- [48] Sloot, W. and Gramsbergen, J. (1994) *Brain Res.* **657**, 124-132.
- [49] Basser, P., Pajevic, S., Pierpaoli, C., Duda, J. and Aldroubi, A. (2000) *Magn. Resonan. Med.* **44**, 625-632.
- [50] Pautler, R. and Koretsky, A. (2002) *Neuroimage* **16**, 441-448.
- [51] Durr, G., Strayle, J., Plemper, R., Elbs, S., Klee, S., Catty, P., Wolf, D. and Rudolph, H. (1998) *Mol. Biol. Cell* **9**, 1149-1162.
- [52] Fleming, M., Trenor, C., Su, M., Foernzler, D., Beier, D., Dietrich, W. and Andrews, N. (1997) *Nat. Genet.* **16**, 383-386.

- [53] Ryu, S., Brown, S., Kolozsvary, A., Ewing, J. and Kim, J. (2002) *Rad. Res.* **157**, 500-505.
- [54] Lin, C., Tseng, W., Cheng, H. and Chen, J. (2001) *Neuroimage* **14**, 1035-1047.
- [55] Lin, C., Wedeen, V., Chen, J., Yao, C. and Tseng, W. (2003) *Neuroimage* **19**, 482-495.
- [56] Pautler, R., Mongeau, R. and Jacobs, R. (2003) *Magn. Resonan. Med.* **50**, 33-39.
- [57] Tindemans, I., Verhoye, M., Balthazart, J. and Van der Linden, A. (2003) *Eur. J. Neurosci.* in press.
- [58] Van Meir, V., Verhoye, M., Absil, P., Eens, M., Balthazart, J. and Van der Linden, A. (2003) *Neuroimage* in press.
- [59] Weissleder, R. (2002) *Nat. Rev. Cancer* **2**, 11-18.
- [60] Budinger, T., Benaron, D. and Koretsky, A. (1999) *Annu. Rev. Biomed. Eng.* **1**, 611-648.